buildings

MDPI

Article

Reconstructing Energy-Efficient Buildings after a Major Earthquake in Hatay, Türkiye

Yousif Abed Saleh Saleh [1], Gulden Gokcen Akkurt [2] and Cihan Turhan [3,*]

[1] Institute of Natural and Applied Science, Atılım University, Ankara 06830, Türkiye; saleh.yousif@student.atilim.edu.tr
[2] Energy Systems Engineering Department, Izmir Institute of Technology, İzmir 35430, Türkiye; guldengokcen@iyte.edu.tr
[3] Energy Systems Engineering Department, Atılım University, Ankara 06830, Türkiye
* Correspondence: cihan.turhan@atilim.edu.tr

Abstract: Türkiye's earthquake zone, primarily located along the North Anatolian Fault, is one of the world's most seismically active regions, frequently experiencing devastating earthquakes, such as the one in Hatay in 2023. Therefore, reconstructing energy-efficient buildings after major earthquakes enhances disaster resilience and promotes energy efficiency through retrofitting, renovation, or demolition and reconstruction. To this end, this study proposes implementing energy-efficient design solutions in dwelling units to minimize energy consumption in new buildings in Hatay, Southern Turkiye, an area affected by the 2023 earthquake. This research focused on a five-story residential building in the district of Kurtlusarımazı, incorporating small-scale Vertical-Axis Wind Turbines (VAWTs) with thin-film photovoltaic (PV) panels, along with the application of a green wall surrounding the building. ANSYS Fluent v.R2 Software was used for a numerical investigation of the small-scale IceWind turbine, and DesignBuilder Software v.6.1.0.006 was employed to simulate the baseline model and three energy-efficient design strategies. The results demonstrated that small-scale VAWTs, PV panels, and the application of a green wall reduced overall energy use by 8.5%, 18%, and 4.1%, respectively. When all strategies were combined, total energy consumption was reduced by up to 28.5%. The results of this study could guide designers in constructing innovative energy-efficient buildings following extensive demolition such as during the 2023 earthquake in Hatay, Türkiye.

Keywords: residential buildings; vertical-axis wind turbine; PV panels; green wall; earthquake; energy-efficient design

check for updates

Citation: Saleh, Y.A.S.; Gokcen Akkurt, G.; Turhan, C. Reconstructing Energy-Efficient Buildings after a Major Earthquake in Hatay, Türkiye. *Buildings* **2024**, *14*, 2043. https://doi.org/10.3390/buildings14072043

Academic Editor: Apple L.S. Chan

Received: 6 June 2024
Revised: 24 June 2024
Accepted: 28 June 2024
Published: 4 July 2024

Copyright: © 2024 by the authors. Licensee MDPI, Basel, Switzerland. This article is an open access article distributed under the terms and conditions of the Creative Commons Attribution (CC BY) license (https://creativecommons.org/licenses/by/4.0/).

1. Introduction

Türkiye's earthquake zone, primarily situated along the North Anatolian Fault, is one of the most seismically active regions in the world, experiencing frequent and sometimes devastating earthquakes [1]. The country's unique tectonic setting requires stringent building codes and continuous advancements in earthquake-resistant construction techniques to protect its population and infrastructure. Therefore, reconstructing energy-efficient buildings after major earthquakes involves integrating resilience with sustainability to create structures that not only withstand future seismic events but also minimize energy consumption [1]. To this end, the Republic of Türkiye's Ministry of Environment, Urbanization and Climate Change announced the "Earthquake Resistance and Energy Efficiency in Public Buildings Project", which aims to retrofit and/or design public buildings, such as educational institutions, dormitories, hospitals, and administrative offices, to enhance their earthquake resilience and improve their energy efficiency [2]. Another goal of the project is to raise awareness by developing a model to achieve energy efficiency in all residential buildings in Türkiye following the project's completion.

In the Hatay earthquake (two earthquakes with magnitudes of 7.2 and 7.1), a total of 80,323 buildings were destroyed, and more than 270,000 buildings were damaged.

Additionally, of the 563,751 people who left Hatay after the earthquake, 434,216 have returned (Figure 1). Therefore, reconstructing and designing new buildings should begin with a comprehensive assessment of the site to understand the specific seismic risks and local climate conditions.

Figure 1. Satellite images before and after the earthquake in Hatay (taken from Google Satellite).

From a design point of view, utilizing advanced materials and construction techniques, such as reinforced concrete and steel frames, ensures structural integrity, which is discussed in the next-generation performance-based seismic design procedures and guidelines for application to new and existing buildings, under the scope of the ATC58 project [3]. On the other hand, developing an overarching framework that enables the consideration of both earthquake resistance and energy efficiency perspectives is highlighted in [4]. Therefore, incorporating insulation, energy-efficient windows, and renewable energy systems such as solar panels enhances the energy performance of new buildings after demolition [5,6]. Additionally, incorporating green roofs and walls can improve insulation and reduce the urban heat island effect. Overall, the goal of reconstructing energy-efficient buildings in earthquake zones is to create buildings that are sustainable and capable of providing long-term energy savings, contributing to both environmental and economic resilience.

Türkiye is now the 16th largest energy consumer, with an average annual growth in electricity consumption of 5% over the last 20 years [7]. Currently, only 20% of total energy consumption is met by electricity, indicating that this growth trend is expected to continue, increasing by 3–4% per year over the next two decades [8]. Türkiye relies heavily on fossil fuel imports, which make up 90% of its total primary energy supply. Consequently, the government is exploring practical methods to satisfy the rapidly increasing energy demand using local renewable sources [9–15]. While Türkiye is a global leader in geothermal energy, its resources fall short of meeting its requirements [16,17]. Despite wind and solar energy contributing around 20% to the total energy production in 2023, Türkiye still has untapped potential in these resources [12,13]. Achieving temporal and geographical flexibility in the power system requires various solutions, depending on the nature of the system and the availability of wind and solar energy, as outlined in a report prepared for the G20 by the International Renewable Energy Agency (IRENA) [18].

Figure 2 illustrates that the share of onshore wind energy constitutes 24% of energy generated by wind turbines. These turbines exploit kinetic energy from the wind turbine and convert it into electrical energy. It is also important to point out offshore wind energy, which comprises a higher percentage of onshore wind energy, an increase of 5%, bringing the total onshore and offshore energy to about 53%. Solar photovoltaic energy is an important part of renewable energy due to the abundance of solar energy available globally, cnostituting approximately 10%.

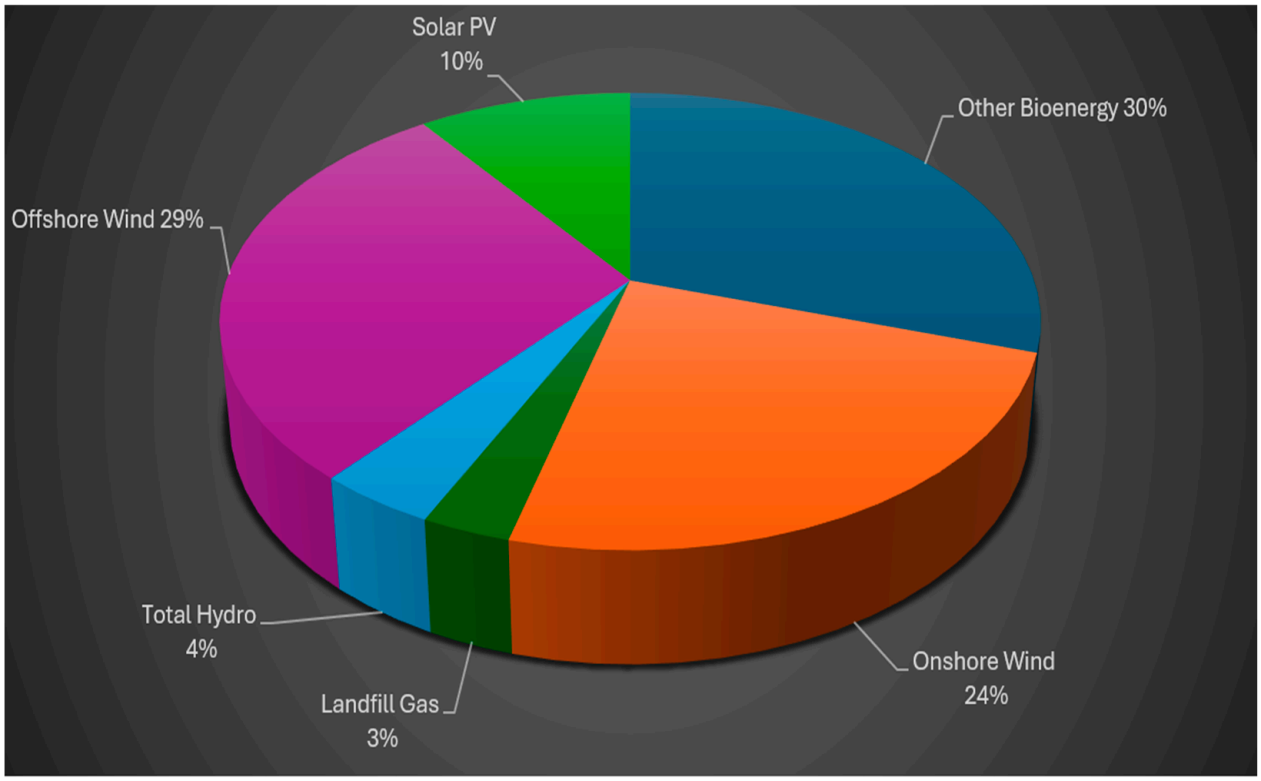

Figure 2. Renewable energy sources (figure developed by the authors).

Several studies have been conducted to assess and improve construction practices in earthquake-prone areas. For instance, Leventeli et al. [1] discussed the importance of constructing buildings on rocky grounds in earthquake-prone areas, citing reduced damage and casualties during earthquakes in Türkiye, prioritizing rocky terrains for construction to mitigate earthquake risks effectively. Varolgüneş [19] explored permanent housing following the 2003 Bingöl earthquake, emphasizing flaws in planning and execution. This underscores the importance of aligning housing designs with local needs for improved resident satisfaction. Yön [20] investigated failure mechanisms in unreinforced masonry buildings after Türkiye's 2019 earthquake, identifying critical structural weaknesses and inadequate connections. The study suggests reinforcement strategies such as shotcrete and fiber-reinforced polymer to enhance building resilience. Ozmen [21] reviewed methods to reduce earthquake damage in Türkiye, advocating for improved civil engineering practices. The study stressed the importance of comprehensive engineering assessments, specialized training for engineers, and heightened public awareness to strengthen earthquake preparedness and mitigation. Işık et al. [22] studied how site-specific design spectra affect building responses to earthquakes in Türkiye's Marmara Region. The paper pointed out the significant impact of local soil conditions on seismic resilience, suggesting the need for tailored building designs to improve earthquake preparedness and structural safety.

Aman and Aytac [23] focused on determining safe post-earthquake assembly areas in Istanbul using a multi-criteria decision-making model and GIS. The authors identified 107 safe assembly areas across seven neighborhoods, considering factors like geology,

hydrology, and accessibility, to enhance urban disaster resilience. Atmaca et al. [24] discussed the performance of masonry and reinforced concrete buildings in Türkiye 's major earthquakes from 1992 to 2020. They linked observed damages to lapses in construction and outdated codes, stressing the need for the rigorous application of updated seismic regulations to reduce future earthquake damage.

Recent seismic events in southeastern Türkiye, particularly the devastating earthquakes of 6 February 2023, have prompted a re-evaluation of the region's preparedness and resilience. Several researchers have scrutinized the seismic performance of infrastructure, with several studies focusing on vulnerabilities in buildings. Among these, Ozturk et al. [25] investigated the seismic performance of school buildings in southeastern Türkiye, and revealed extensive damage due to outdated seismic codes, poor material quality, and inadequate structural details. The research stressed the need for retrofitting and stricter adherence to modern seismic regulations to prevent future damage. Ozturk et al. [26] analyzed the impacts of significant seismic events, revealing extensive damage to reinforced concrete buildings. They noted that numerous structures did not comply with the seismic codes applicable at their time of construction and were situated in high-risk areas, resulting in catastrophic outcomes. Tao et al. [27] explored building damage in Hatay due to the 6 February 2023 earthquakes. They noted extensive damage from the quakes, which were intensified by side-effects like liquefaction and over-design ground motions. The study emphasized the resilience of well-constructed buildings and the catastrophic failures of those not up to seismic standard. However, to the best of the authors' knowledge, there is very limited research on reconstructing buildings with a focus on energy efficiency after major earthquakes.

On the other hand, employing energy-efficient building design strategies is common in the literature. Numerous recent studies have been carried out involving wind energy, solar energy, and green walls toward reducing energy consumption in buildings. For instance, Alrwashdeh [28] examined the impact of PV panel orientation (landscape and portrait) in Amman, Jordan, by using 3D energy v.2020 simulation software. They found that the landscape orientation generated 13.7% more energy than the portrait orientation. This difference happened because of reduced energy losses from blocking and shading between panels in the landscape orientation. Burg et al. [29] discussed the effect of PV panel systems in urban climates, installing high-efficiency PV panels outside urban regions to reduce environmental impact. Biyik et al. [30] and Maghrabie et al. [31] both presented "*Building-integrated photovoltaic systems BIPV*" and found that the extent of the impact of these types of solar cells and their ability to reduce energy consumption in buildings make them valuable for improving the design of sustainable buildings. This study also indicated how to enhance technology and economic incentives. Topal et al. [32] and Çeçen et al. [33] introduced the importance of PV panels in Türkiye because of its geographical location and the promotion of the use of solar energy; both studies indicate an increased demand for this type of energy to reduce dependence on fossil fuels and the urgent need for the government sector to support this technology to achieve environmentally friendly buildings.

Hajizadeh and Seyis [34] investigated the retrofitting of a residential building in Antalya, Türkiye, using different methods such as PV panels, wall insulation, and other strategies. They found a reduction in total energy consumption of 58%. This study shows the possibility of applying this type of strategy in Mediterranean climates. Adan and Filik [35] integrated 3 KW solar PV systems in Eskişehir, Türkiye, which has higher solar potential than many European regions. These PV panels produced 4839 KWh/year with a performance value of 84.8%. Turhan and Saleh [36] performed a simulation study by integrating forty small-scale IceWind turbines mounted on the roof of a building in a case study in Istanbul, Türkiye, and decreased annual energy by 9.3%.

To the best of the authors' knowledge, there are limited studies that incorporate energy-efficient design strategies for reconstructing new buildings following major earthquakes. This study also introduces a novel approach by designing a small-scale wind turbine to be

installed on the rooftop of a building and implementing thin-film PV panels and a green wall on the structure.

2. Methods

A case building in Hatay, Turkey, was selected to implement three strategies. Initially, the building was simulated without utilizing any solutions, and the energy consumption of the baseline model was calculated, including total energy like fuel consumption and electricity. Subsequently, this research explored three strategies separately: thin-film PV panels, IceWind turbines, and green walls. Finally, the results were compared to determine the effectiveness of each strategy in significantly reducing energy consumption in the case building. Figure 3 illustrates a flow chart of this study.

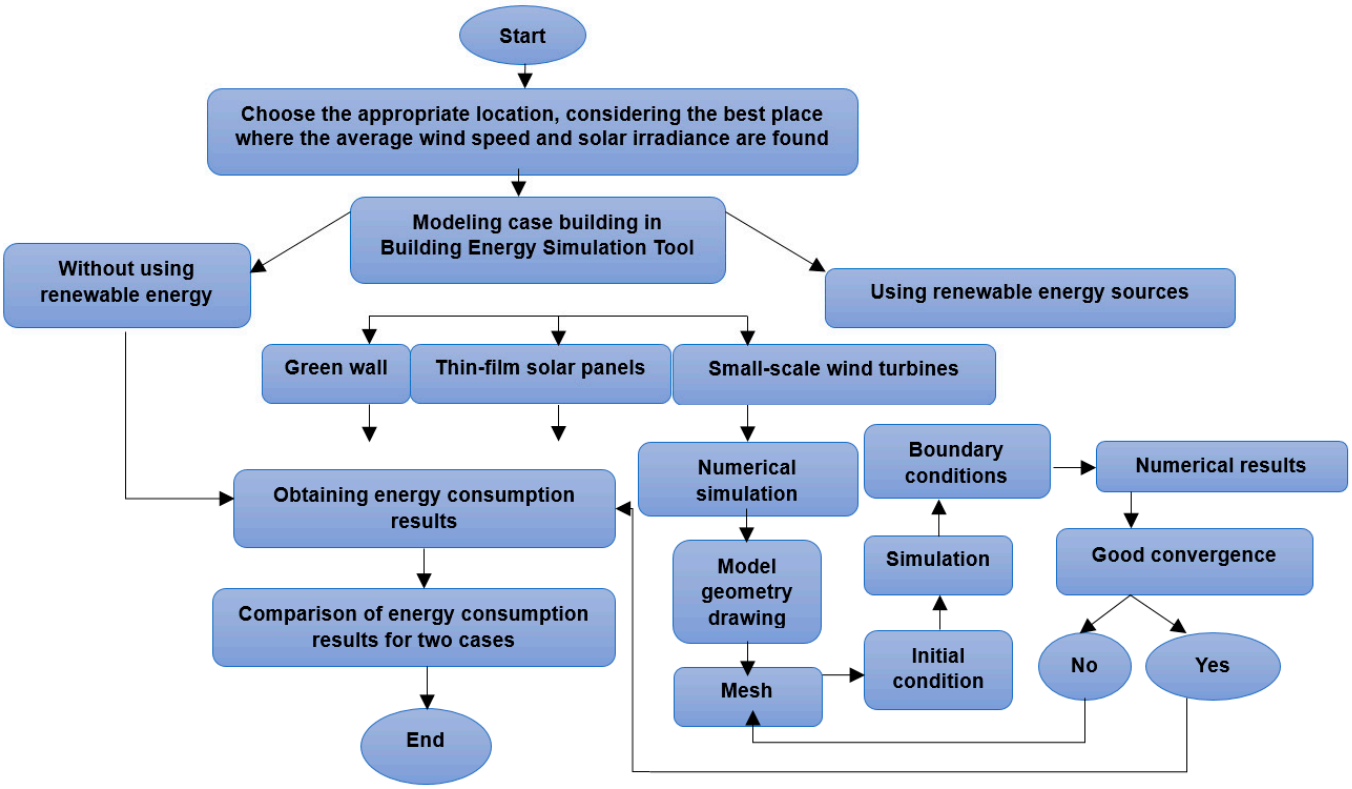

Figure 3. Flow chart of the study.

2.1. Climate and Location Analysis

Hatay, situated in Southern Türkiye at coordinates (latitude 36° N, longitude 36° E), falls within the Csa-type (temperature) climate zone according to the Köppen–Geiger climate classification, a fundamental tool in climatology [37]. The Kurtlusarımazı district in Hatay was selected for this study due to its favorable conditions, characterized by abundant sunlight and wind. Figure 4 depicts the locations of Hatay and Kurtlusarımazı.

Figure 5 displays a distribution heat map of Hatay city, highlighting areas with varying solar energy potential. Regions with low potential are depicted in blue, those with medium radiation in yellow, and areas inclined towards orange indicate a high capacity for solar energy, making them ideal for solar cell utilization. Therefore, Kurtlusarımazı stands out as one of the regions with a significant abundance of solar energy.

Figure 4. Locations of Hatay and Kurtlusarımazı districts.

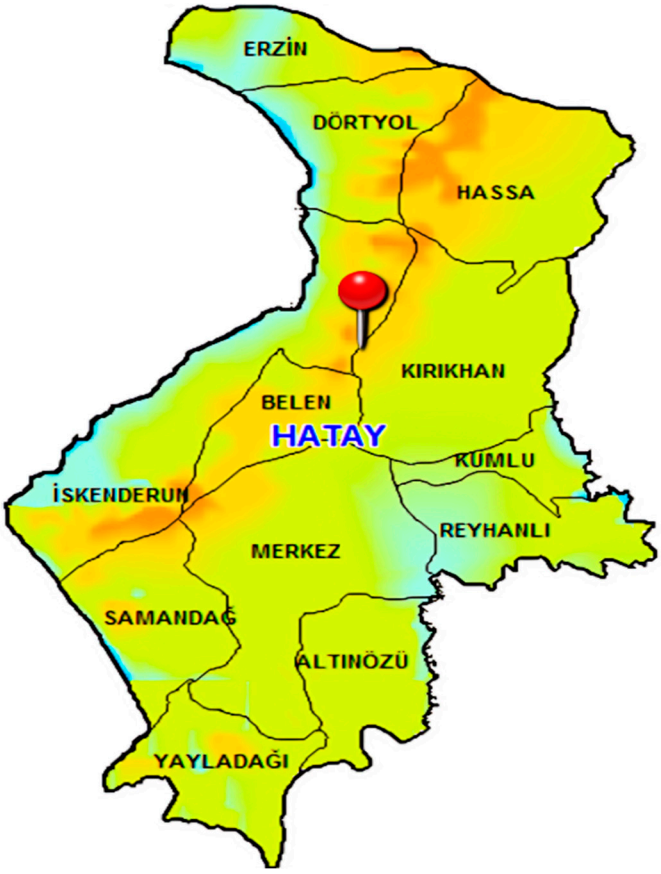

Figure 5. Solar energy potential map of Hatay [38].

Kurtlusarımazı is situated in a region known for high winds, as shown in Figure 6, where wind speeds can reach up to 10 m/s due to the area's elevated position above sea level. The wind energy potential around this region was assessed using the Atlas website [39], with red indicating a high level of wind energy potential. The graph illustrates that the highest wind speeds are observed at the initial measurement point, corresponding to periods of intense wind activity. Subsequently, there is a noticeable and consistent decrease in wind speed, attributed to seasonal transitions and meteorological influences impacting the area consistently.

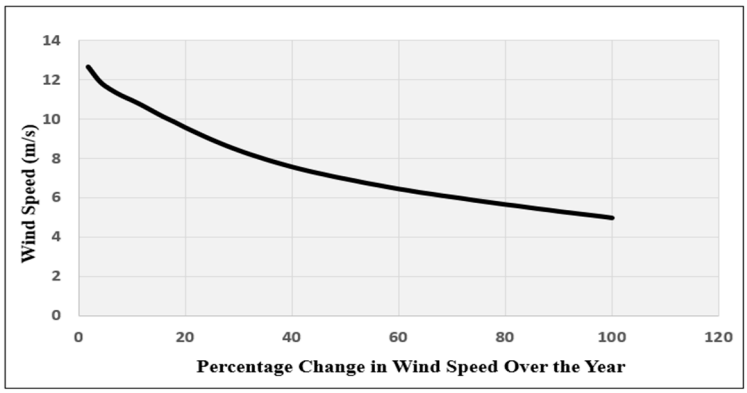

(**a**)

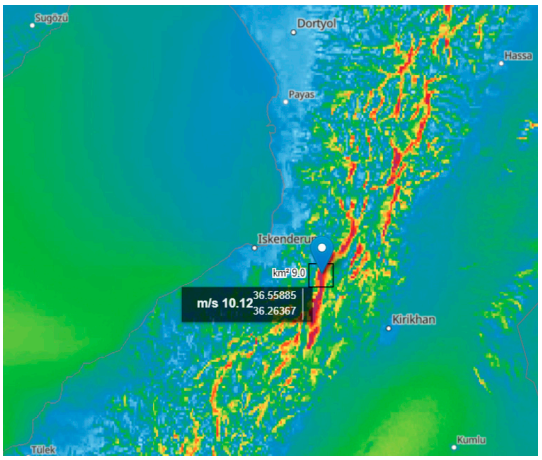

(**b**)

Figure 6. Climate analysis of wind energy: (**a**) annual wind speed curve [39]; (**b**) wind energy potential [39].

2.2. Case Building Design

The case building is a residential structure located in the Kurtlusarımazı district of Hatay, Turkey. Illustrated in Figure 7, the building comprises five stories, each housing two apartments. Each apartment is configured with three bedrooms, two bathrooms, a living room, a kitchen, an entrance, two balconies, and storage space. The total area of the case building measures 424 square meters, with its parameters derived from the architectural drawings of the building. Table 1 provides an overview of the design criteria and features of the case study building, sourced from [40].

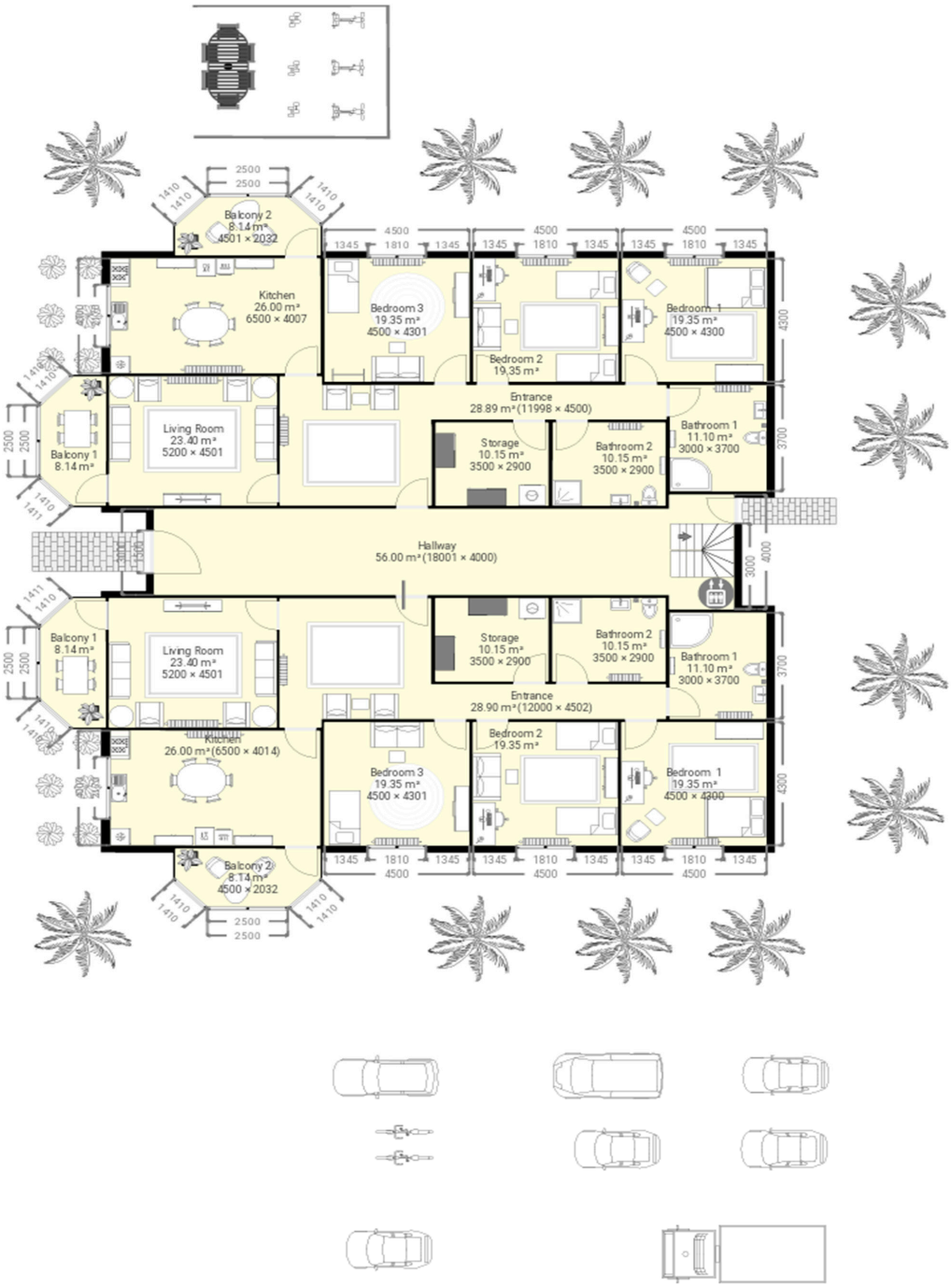

Figure 7. Architectural drawings of the residential plan.

Table 1. Basic design features.

The Building Construction Properties	Baseline Model
Number of floors	5
Overall floor area	424 m^2
Number of spaces	115
External walls (U-value)	0.35 (W/m^2K)
Internal walls (U-value)	1.923 (W/m^2K)
Roof (U-value)	0.25 (W/m^2K)
Ground floor (U-value)	0.25 (W/m^2K)
Glazing type + U-value	Reference glazing with 1.978 (W/m^2K)

The external wall layers in the base design are composed of gypsum plaster (0.03 m thickness, 0.4 W/mK) thermal conductivity), XPS extruded polystyrene (0.07 thickness, 0.034 W/mK thermal conductivity), concrete block (0.1 m thickness, 0.013 W/mK thermal conductivity), and gypsum plaster (0.02 m thickness, 0.4 W/mK thermal conductivity). The exterior walls have a U-value of 0.35 W/m^2K.

2.3. Energy Simulation Analysis

An hourly dynamic building simulation tool, DesignBuilder, was used to simulate the baseline model and energy-efficient design strategies [41]. The materials for the case building were obtained from an architectural drawing, and the construction model was based on the values as in Table 1.

Figure 8 represents the baseline model in three dimensions. The case building was modeled with trees for accurate results, via shading effects and simulated weather data from LARNACA-CYP IWEC. The simulation includes four scenarios, the first one without any solution and other cases with PV panels, small-scale wind turbines, and a green wall, sequentially.

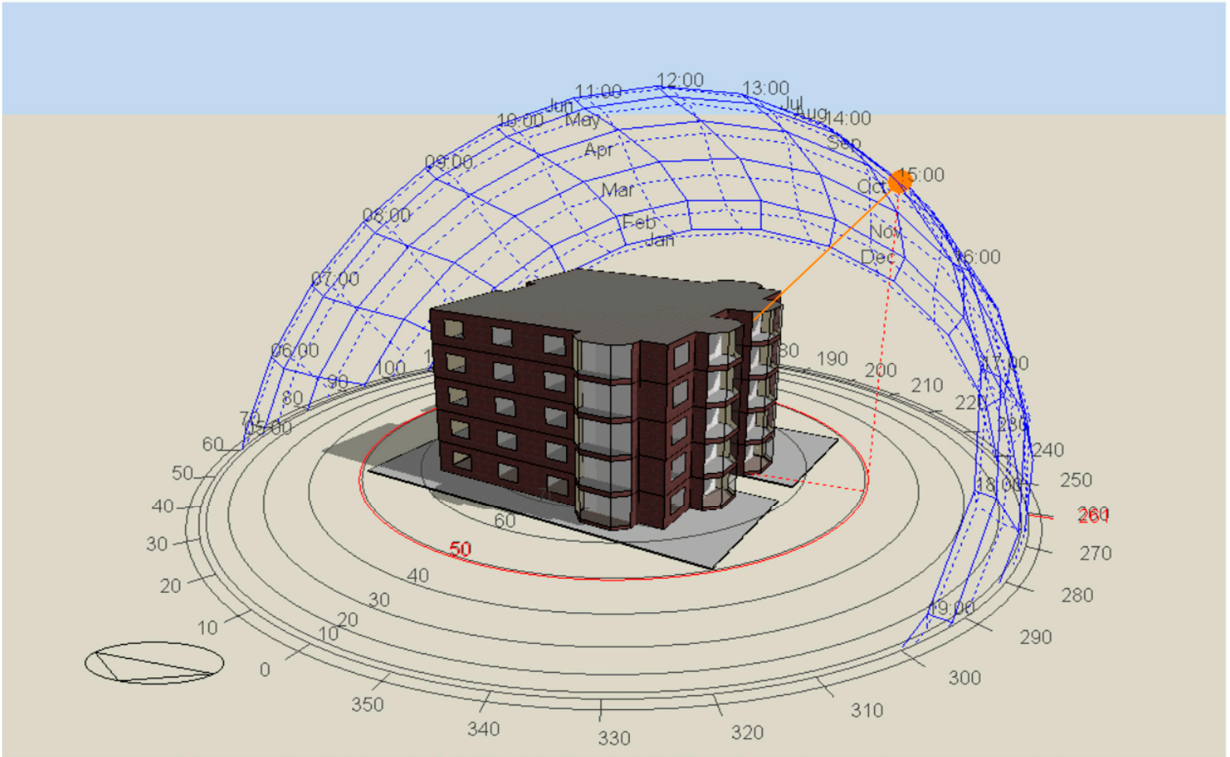

Figure 8. Building energy simulation model of the case building.

2.4. Retrofitting Strategies

Three energy-efficient design strategies were conducted for the case building. The aim of implementing energy-efficient design strategies was to examine the impact of these solutions on decreasing the energy consumption of residential buildings and reducing environmental pollution by using sustainable energy. It is significant to remember that on-grid systems are used for cases one and two since they involved lower initial investments as there was no need for energy storage solutions.

2.4.1. Case One: Adding Photovoltaic (PV) Panels

Photovoltaic PV panels are installed around two big circles and into the walls to the south of the building in order to achieve the maximum possible benefit from capturing solar energy (Figure 9). A thin-film G × B 500 Bifacial PV module is used in the case building, which was designed to capture sunlight from both the front and back, boosting energy efficiency by up to 20%. The power output ranges between 19.3% and 23.2% with added backside power. Due to its heat resistance, this thin-film PV panel is significantly effective in hot climates because these panels are built to endure temperature ranging from 40 to +85 °C. Additionally, they can handle heavy snow and wind loads. Table 2 includes all thin-film PV module specifications.

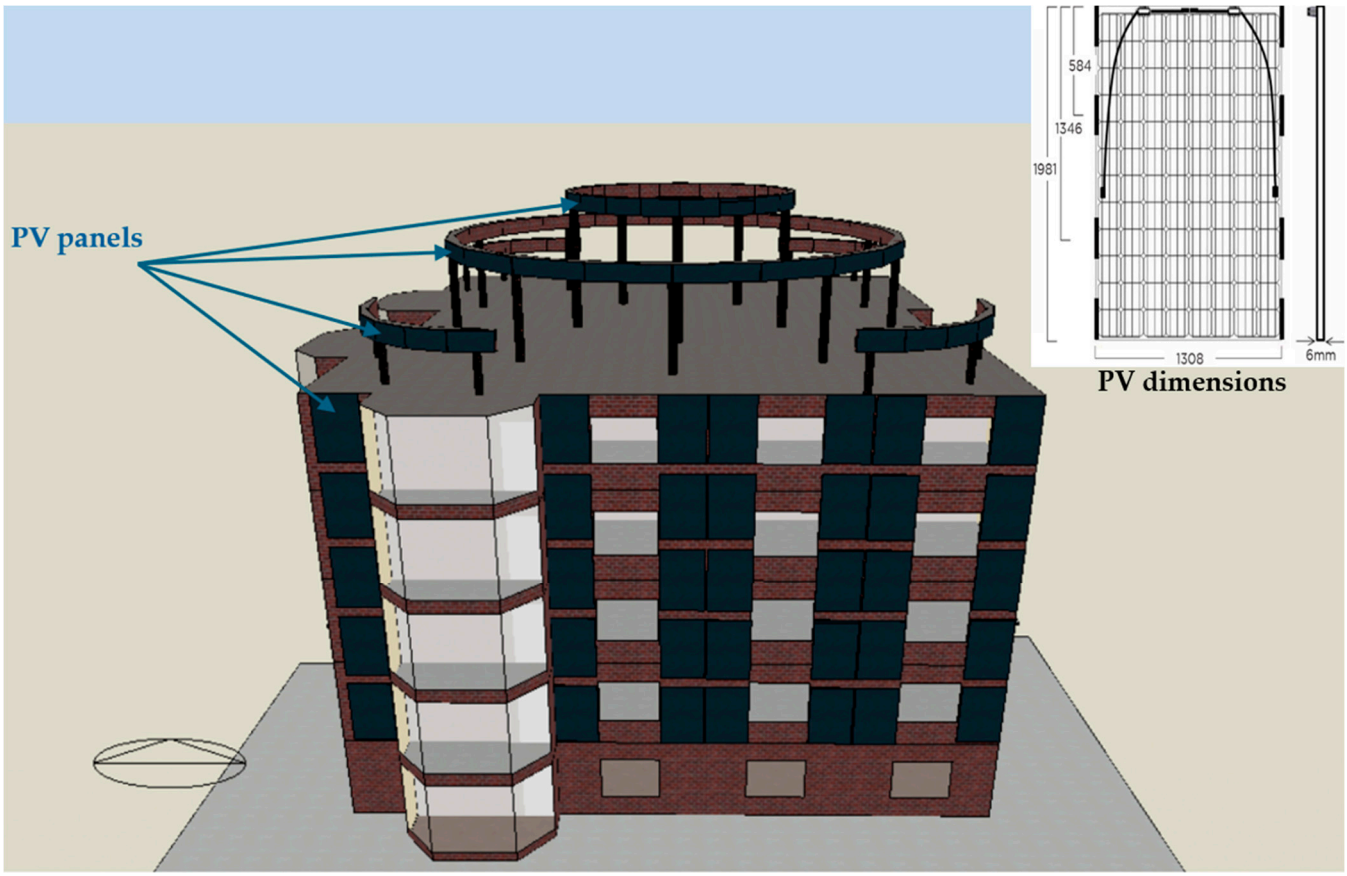

Figure 9. Thin-film G × B 500 Bifacial PV module mounted on the case building.

2.4.2. Case Two: Building-Integrated Wind Turbine Design

A small-scale IceWind turbine was designed for the case building. Forty-two IceWind turbines were used on the roof of the building and distributed in a way that was proportional to the available space on the case building's rooftop to ensure that they captured the maximum possible level of wind energy, taking into account the distance between the turbines in a manner that would not affect the aerodynamics between each turbine

and its neighboring turbines. The final IceWind turbine blade used in this research was designed using Solidworks Software v.2018 [42]. It features dimensions with a diameter (D) of 0.7575 m and a height (H) of 1.456 m, with a swept area of 1.95 m^2, which was calculated directly from Solidworks. Figure 10 illustrates the design of the three-blade IceWind VAWT.

Table 2. PV module specifications (the data are taken from https://energypal.com/best-solar-panels-for-homes/sunpreme/gxb-500, accessed on 23 June 2024).

Photovoltaic Properties		**Photovoltaic Properties**	
Cell type	Bifacial Hybrid Cell Technology (HCT)	Rated electric power output per module (W)	500
Cells in series	96	Short-circuit current (A)	9.3
Active area m^2	2.591148	Module current at max power (A)	8.8
Total area of PV panels (m^2)	148.2	Temperature coefficient of short-circuit current (A/K)	0.00372
Transmittance absorptance product	0.9	Module voltage at max power (V)	57.4
Semiconductor bandgap (eV)	1.12	Open-circuit voltage (V)	72.9
Reference temperature (°C)	25	NOCT cell temperature (°C)	45
Reference insolation (W/m^2)	1000	NOCT ambient temperature (°C)	20
Module heat loss coefficient (W/m^{-2} K)	30	Temperature coefficient of open-circuit voltage (V)	−0.17496
Rated electric power output per module (W)	500		

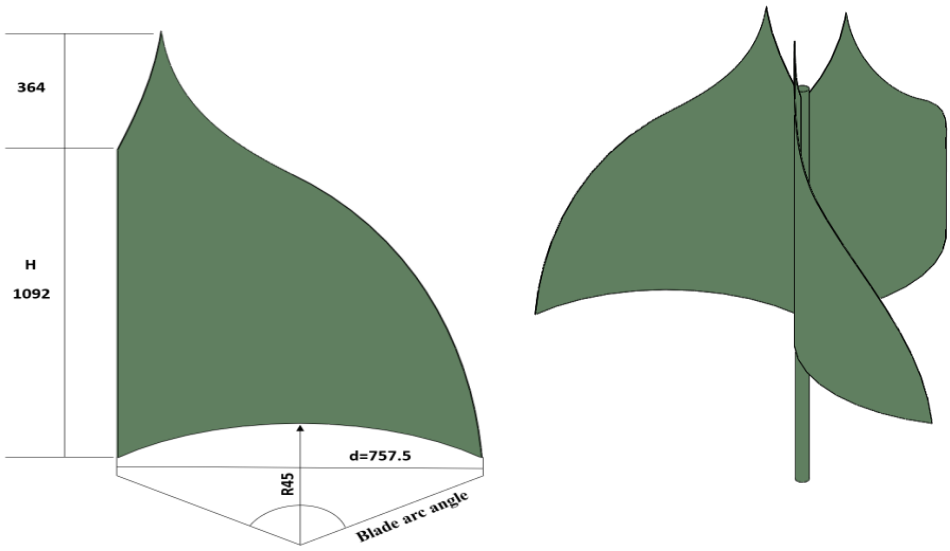

Figure 10. IceWind blade (dimensions in mm).

Figure 11 shows two concrete circles on top of the case building supported by columns proportional to the size of the circle. Ten IceWind turbines are shown on the smaller circle and twenty others on the larger circle. In addition, 12 IceWind turbines were placed distributed over the four corners of the building in order to reduce energy consumption in the case study building.

Air flow simulations around the IceWind turbine were performed with a 3D domain with dimensions of 6 m × 3 m × 3 m in ANSYS Fluent Software v.R2. [43]. The physical model includes a velocity inlet boundary where wind enters at speed of 10 m/s, a pressure outlet where the existing air is removed, and no-slip boundary conditions on all the other surfaces.

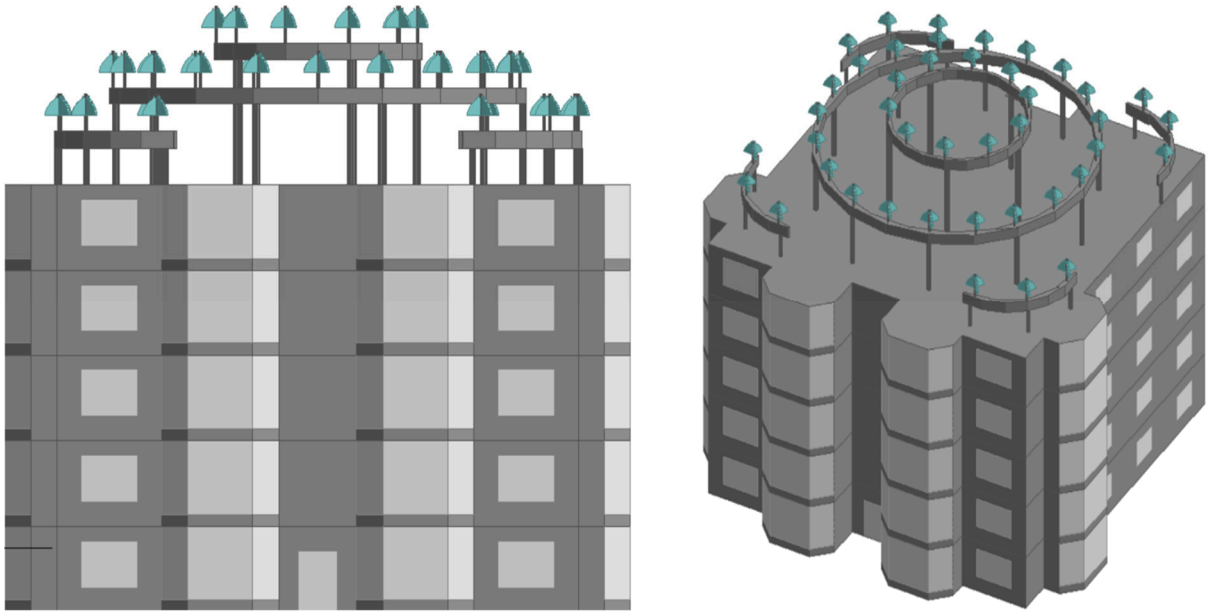

Figure 11. IceWind turbines mounted on the building (developed by the authors).

The mesh used in the simulation is a tetrahedral mesh, while the nodes include 861,882 and 4,790,485 elements. This higher mesh was selected for better accuracy of the results. The study utilized the Shear Stress Transport (SST) K-ω model, which has been described to be more exact in terms of the aerodynamic performance of such VAWTs [44,45]. Figure 12 illustrates the boundary conditions and the mesh of the IceWind turbine domain from a side view.

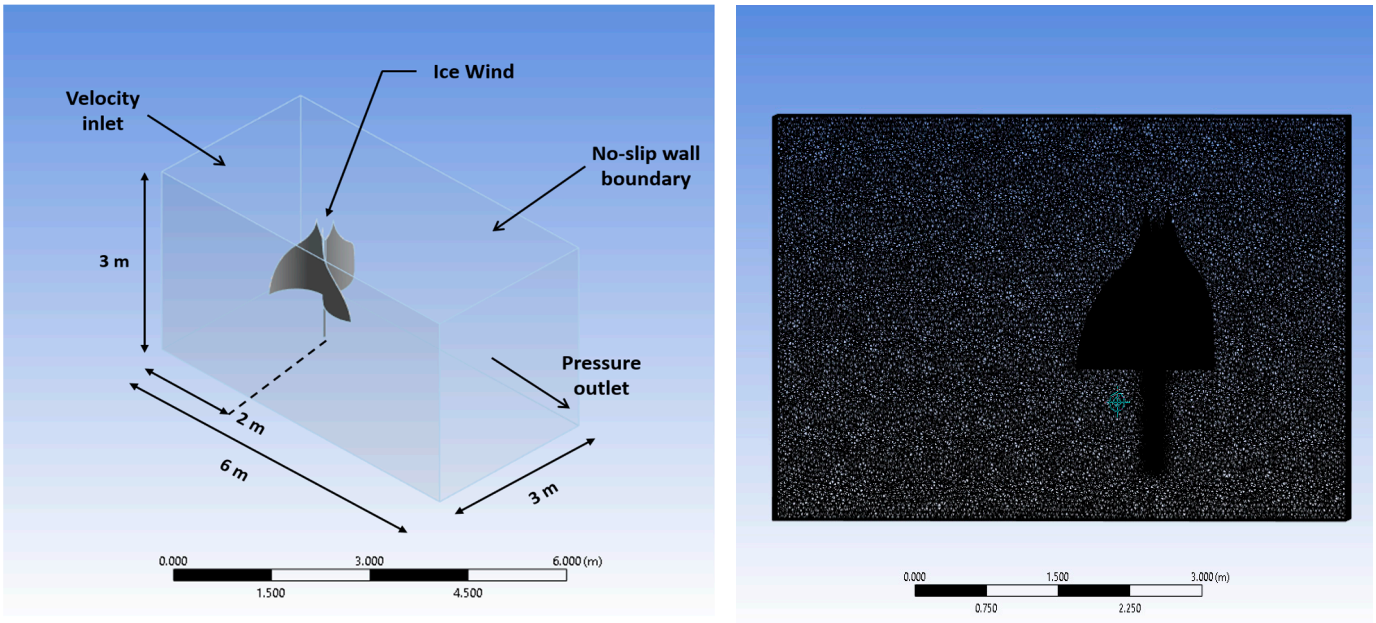

(**a**) (**b**)

Figure 12. IceWind model in ANSYS: (**a**) IceWind turbine and domain dimensions (m); (**b**) mesh of the IceWind turbine domain from side view.

The average wind speed was taken as 10 m/s, as mentioned before for the Kurtlusarı-mazı location. After performing the simulation, we found that the rated power output was 305 watts with a rotor speed of 190 rev/min and a tip speed ratio of 1.51. Table 3 presents the input parameters for the building-integrated wind turbines using DesignBuilder Software.

Table 3. Input parameters of wind turbine (the data are taken from DesignBuilder and Fluent).

Input Parameter		Input Parameter	
Operation type	24/7	Cut-out wind speed (m/s)	25
Rotor type (rev/min)	Vertical Axis Wind Turbine	Cut-in wind speed (m/s)	3.5
Rotor diameter (m)	1.515	Maximum tip speed ratio	1.51
Number of blades	3	Maximum power coefficient	0.26
Rated power output (W)	305	Annual local average wind speed (m/s)	10
Rated wind speed (m/s)	10	Power control	Fixed-speed variable-pitch

Transport equations are used to calculate the turbulent kinetic energy (Equations (1) and (2)):

$$\frac{\partial}{\partial t}(\rho k) + \frac{\partial}{\partial x_i}(\rho k u_i) = \frac{\partial}{\partial x_j}\left(\Gamma_k \frac{\partial k}{\partial x_j}\right) + G_k + Y_k + + S_k + G_b \quad (1)$$

$$\frac{\partial}{\partial t}(\rho \omega) + \frac{\partial}{\partial x_i}(\rho \omega u_i) = \frac{\partial}{\partial x_j}\left(\Gamma_\omega \frac{\partial \omega}{\partial x_j}\right) + G_\omega + Y_\omega + + S_\omega + G_{\omega b} \quad (2)$$

It is worth noting that the equations for the calculation of turbulent kinetic energy are proposed by the authors. In these two equations, G_k is the turbulent kinetic energy due to mean velocity gradients. G_ω denotes the generation of ω. Γ_k and Γ_ω refer the effective diffusivity of k and ω, respectively. Y_k and Y_ω symbolize the dissipation of k and ω, respectively, due to turbulence. G_k and $G_{\omega b}$ account for buoyancy terms. S_k and S_ω are defined by the user as source terms [45].

The power coefficient, toque coefficient, tip speed ratio, and wind turbine efficiency are obtained from the following equations, respectively:

$$C_P = \frac{P_{Turbine}}{P_{available}} = \frac{P_{Turbine}}{0.5\rho A_S V^3} \quad (3)$$

$$C_T = \frac{T}{0.5\rho A_S V^2 R} \quad (4)$$

$$\lambda = \frac{\omega R}{V} \quad (5)$$

$$\eta = \frac{P_{Turbine}}{0.5\rho A_S V^3} \times 100\% \quad (6)$$

where:

$P_{Turbine}$: power output (watts).
ρ: air density (kg/m^3).
A_S: swept area (m^2).
V: wind speed (m/s).
T: torque (N.m).
R: radius of the rotor (m).
ω: angular velocity (rad/s).

2.4.3. Case Three: Green Structure Applications

To measure the effects of green system installations, the ivy species Hedera Canariensis Gomera is applied to the residential building. This plant is used as it grows easily in the Hatay region, making it suitable for assessing the impact of such applications.

Additional layers employed in the baseline model for the purpose of the green walls are shown in Figure 13 below. It should, however, be noted that after the applying soil, a 200 mm thick vegetation layer is incorporated. It consists of an 89 mm overlaid air gap, 10 mm PVC, 50 mm wool fiber slab, 200 mm of cultivated peat soils, and a 200 mm vegetation layer over the present wall's layers.

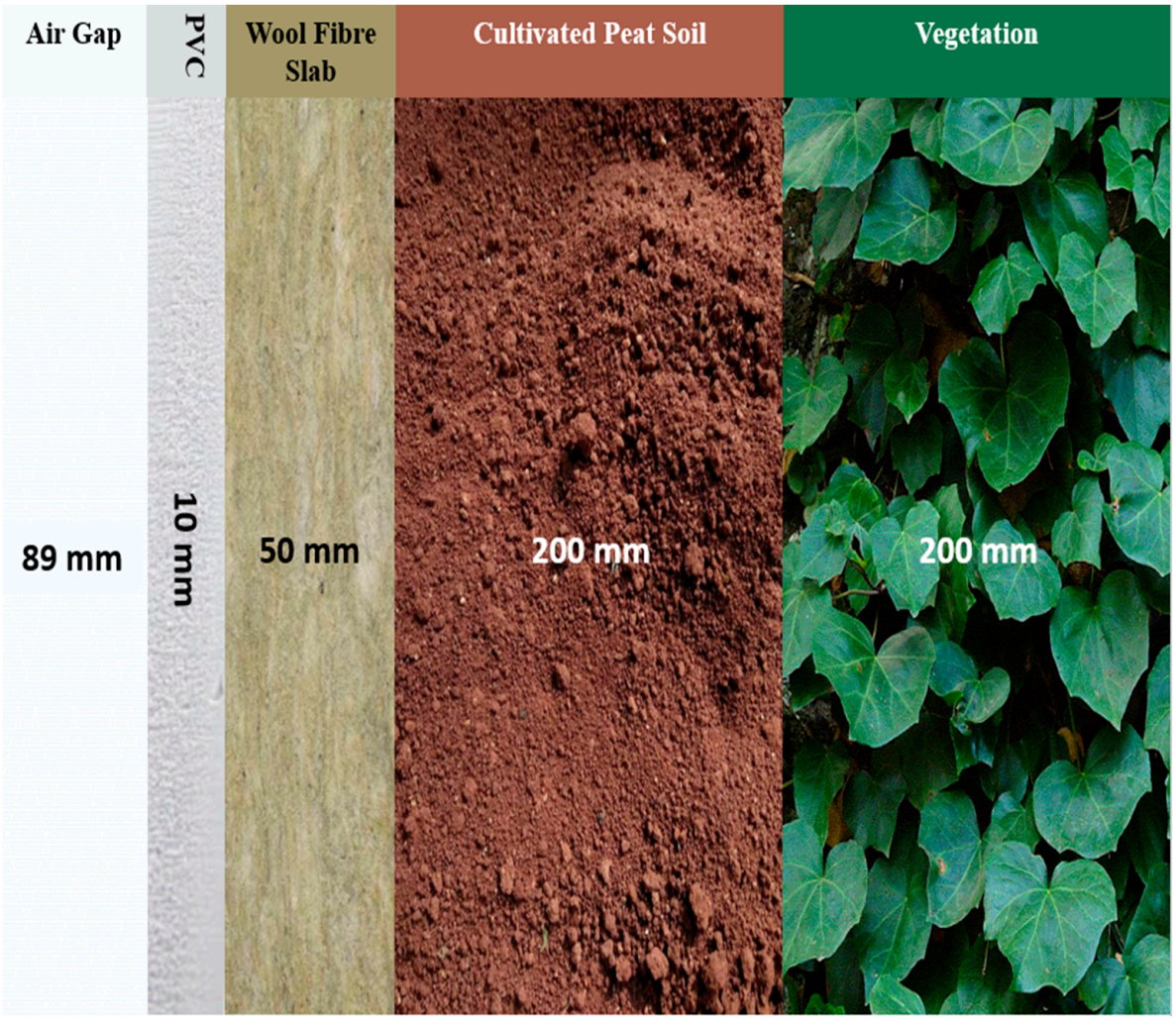

Figure 13. Layers of green structure (developed by the authors).

Table 4 displays the characteristics of *Hedera Canariensis Gomera*, which are utilized as input data for the wall in DesignBuilder Software.

Table 4. Specifications for green wall plant (the data are adopted from DesignBuilder).

Input Parameter		Input Parameter	
Conductivity (W/mK)	0.4	Leaf Reflectivity	0.22
Specific Heat (J/kgK)	1100	Leaf Emissivity	0.95
Density (kg/m^3)	641	Max. Vol. Moisture Cont. Sat.	0.5
Height (m)	0.1	Min Residual Vol. Moist. Content	0.01
Leaf Area Index (LAI)	2.7	Initial Vol. Moist. Content	0.15
Min. Stom. Res. (s/m)	180		

Hedera Canariensis Gomera is used for three sides of the case building, except in the south direction due to the PV panels. With this plant's ability to climb, it can easily grow in these climates and dry temperatures. Figure 14 below shows the application of the plant to three sides of the building.

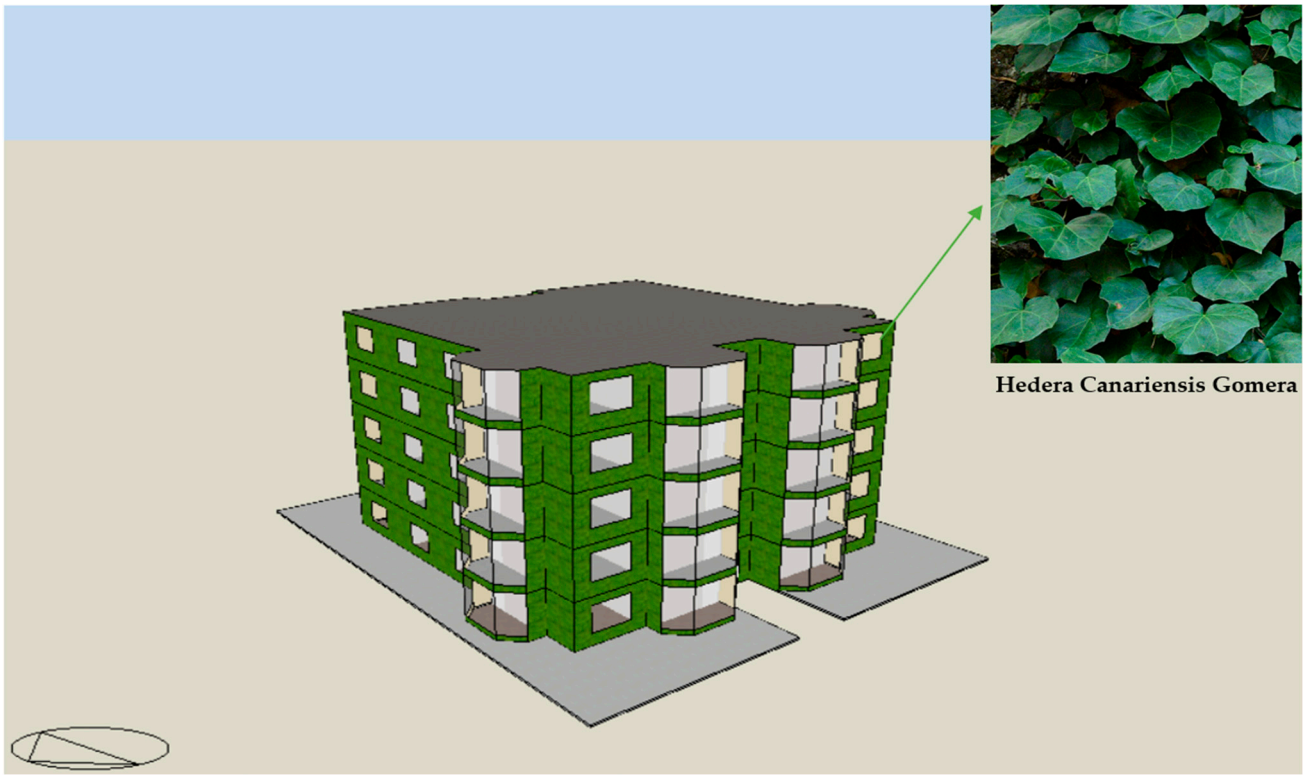

Figure 14. Green wall for three sides of building except in the south direction.

3. Results and Discussion

Table 5 depicts the annual meteorological data for the Kurtlusarımazı/Hatay zone used in the simulations.

Table 5. Meteorological data results of Kurtlusarımazı/Hatay.

Parameters	Unit	Maximum	Median	Minimum
Air temperature	°C	35	20	5
Wind speed	m/s	12	10	3
Total solar radiation	kWh/m^2 day	1700	1650	1514

Therefore, the power of each wind turbine is computed as 305 watts with a 1.95 m^2 swept area for each turbine and a 190 rev/min rotor speed. The torque of each wind turbine is 15.533 N.m.

We performed an analysis of the distribution of dynamic pressure and velocity magnitude, along with the flow streamlines, surrounding the turbine blades under a wind velocity of 10 m/s. Figure 15a,b show 3D and 2D representation of the turbine with a dynamic pressure with a scale ranging from 0.00107 Pa to 254 Pa. The 3D and 2D velocity magnitude of the airflow is shown, with a 19.8 m/s maximum speed, focusing on the velocity magnitudes near the turbine blades and the surrounding area.

After integrating all cases as discussed previously in Section 3, the results obtained for each case are shown in Table 6.

The energy consumption of the baseline model was estimated to be 182.4 KWh/m^2 per year. The most effective energy-saving strategy was found to be PV panels (case1) with an energy consumption decrease of 18% compared to the baseline model. On the other hand, by applying 42 IceWind turbines equipped with three blades, the simulated building's annual energy consumption was determined to be 166.9 kWh/m^2. In other words, by integrating wind turbines into the existing building, energy consumption was

reduced by 8.5% annually. When *Hedera Canariensis Gomera* was used for the walls, this energy-efficient design strategy decreased total energy consumption by 4.1% compared to the baseline model. It is crucial to note that only cooling energy consumption is decreased in this design strategy. On the other hand, when all energy-efficient design strategies were applied together, a 28.5% energy saving was achieved compared to the baseline model. The combined application of green structures, solar panels, and wind turbines offers significant energy savings and efficiency improvements over implementing each technology separately. By leveraging the complementary nature of solar and wind energy, optimizing the use of space, and incorporating energy-efficient building designs, the integrated approach maximizes energy production and minimizes consumption, leading to the most effective and sustainable energy solution.

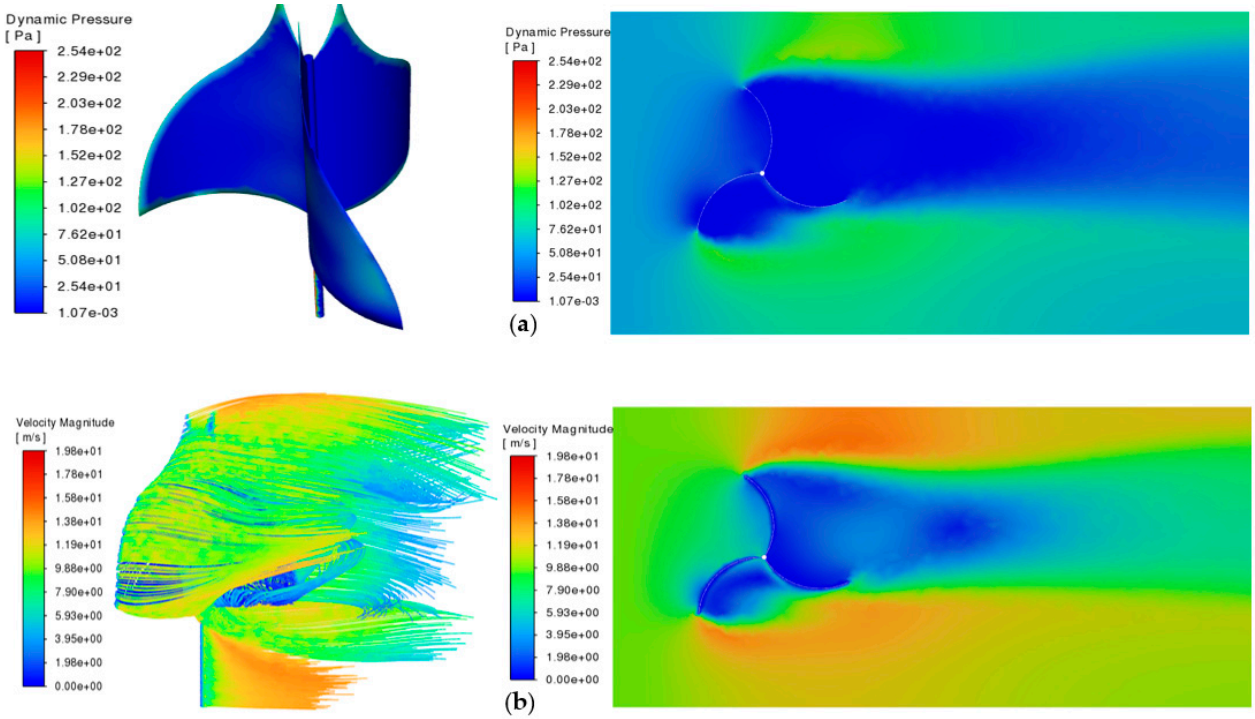

Figure 15. Pressure distributions and velocity magnitude of IceWind turbine: (**a**) dynamic pressure; (**b**) velocity magnitude.

Table 6. Simulation results for all cases.

Model Name	Energy Consumption (kWh/m^2)	Energy Saving %
Baseline model	182.4	-
Case 1	149.6	18
Case 2	166.9	8.5
Case 3	174.9	4.1
All cases together	130.5	28.5

Energy-efficient design strategies such as PV panels, small-scale wind turbines, and the application of green walls play a crucial role in shaping the sustainability of newly designed buildings after major earthquakes. These strategies not only contribute to reducing environmental impact but also offer economic benefits and enhance overall comfort and well-being for occupants. Thin-film PV panels are a popular choice for integrating renewable energy sources into novel building designs. By incorporating PV panels into building designs, architects and engineers can significantly decrease the carbon footprint of buildings and contribute to mitigating climate change. Additionally, advancements in PV technology have led to more efficient and cost-effective solutions, making them

increasingly attractive for new building projects. Regions such as Hatay, Türkiye, have significant potential for implementing thin-film PV panels, as evidenced by the findings of this study.

Small-scale wind turbines are another energy-efficient design strategy that can be integrated into building designs, especially in areas with suitable wind conditions. When combined with PV panels, small-scale wind turbines can further enhance the overall energy production of a building, making it more self-sufficient and reducing reliance on the grid. The novel IceWind turbine design presented in this study could assist designers and architects in creating new energy-efficient buildings.

Green walls offer numerous benefits, including improved air quality, thermal insulation, and aesthetic appeal. From an energy-efficiency perspective, green walls can help regulate indoor temperatures, reduce the heat island effect, and lower the energy required for cooling and heating. Additionally, they contribute to biodiversity and create a healthier and more enjoyable indoor environment for occupants.

Incorporating these energy-efficient design strategies requires careful planning, integration, and optimization to maximize their effectiveness. Factors such as building orientation, climate conditions, site-specific considerations, and local regulations play a crucial role in determining the optimal deployment of PV panels, small-scale wind turbines, and green walls. Collaborative efforts between architects, engineers, sustainability experts, and stakeholders are essential to ensure the successful implementation of these strategies in newly designed buildings.

Overall, energy-efficient design strategies such as PV panels, small-scale wind turbines, and green walls offer a holistic approach to creating sustainable and environmentally friendly buildings. By embracing these technologies and design principles, we can move towards a more energy-efficient and sustainable built environment for the future.

One can question the feasibility of these design strategies. Table 7 depicts the investment and operational costs of these strategies. The pay-back period of the combined strategies is calculated to be 7.4 years considering a local electricity price of USD 0.07 per kWh. Note that labor prices and VAT are included in the table.

Table 7. Economic feasibility analysis for all cases.

Model Name	Energy Saving	Capital Cost (USD per Unit)	Operational Cost (USD per Unit)	Pay-Back Period (Years)
Baseline model	-	-	-	-
Case 1	18	515	20	5.7
Case 2	8.5	2000	50	11.3
Case 3	4.1	758	68	7.1
Combined	28.5	3273	138	7.4

The findings of this study are primarily based on computer simulations due to the earthquake; therefore, it is crucial to validate the data to ensure the results are reliable and accurate. Some approaches to validating the data include field measurements after the construction of the building, comparisons of the data with other simulation tools, and validation through pilot projects in the earthquake zone.

4. Conclusions

This study demonstrated that the effective integration of sustainable energy practices, such as Vertical-Axis Wind Turbines (VAWTs), Photovoltaic (PV) panels, and green walls, significantly reduced energy consumption in residential buildings in Hatay, Türkiye. Through modeling and analysis using ANSYS Fluent and DesignBuilder, the results confirmed the efficacy of these strategies individually and their collective impact as part of an integrated approach.

Integrating PV panels resulted in an 18% reduction in energy consumption, while the use of small-scale IceWind turbines contributed to an 8.5% decrease. Additionally, green wall implementation led to a 4.1% reduction in energy usage. When combined, these strategies achieved a substantial 28.5% decrease in total energy consumption. Moreover, the integrated approach not only reduced energy consumption, but also enhanced environmental quality by leveraging renewable sources over non-renewable ones, including passive and active solutions.

This study sets a precedent for implementing sustainable solutions in urban areas, especially those recovering from disasters such as major earthquakes, while searching for improved energy efficiency. Further research is warranted to explore the long-term effects of these strategies and expand their implementation to diverse climatic and urban settings, aiming to maximize planetary sustainability in residential construction.

Author Contributions: Conceptualization, Y.A.S.S. and C.T.; methodology, G.G.A. and C.T.; software, Y.A.S.S.; validation, G.G.A. and C.T; formal analysis, Y.A.S.S. and C.T.; investigation, Y.A.S.S.; writing—original draft preparation, Y.A.S.S.; writing—review and editing, G.G.A. and C.T.; supervision, C.T. All authors have read and agreed to the published version of the manuscript.

Funding: This research received no external funding.

Data Availability Statement: The raw data supporting the conclusions of this article will be made available by the authors on request.

Conflicts of Interest: The authors declare no conflicts of interest.

References

1. Leventeli, Y.; Yilmazer, O.; Yilmazer, I. The importance of effective land use planning for reduction in earthquake catastrophe. *Arab. J. Geosci.* **2020**, *13*, 1010. [CrossRef]
2. Republic of Türkiye, Ministary of Environment. Urbanization and Climate Change. Available online: https://kamuguclendirme.csb.gov.tr/en/general-information-of-the-project-i-109613 (accessed on 6 June 2024).
3. FEMA. Methodology. In *Seismic Performance of Buildings*; FEMA Publication No. P-58-1; Applied Technology Council: Redwood City, CA, USA, 2012; Volume 1.
4. Calvi, G.M.; Sousa, L.; Ruggeri, C. Energy Efficiency and Seismic Resilience: A Common Approach. In *Multi-Hazard Approaches to Civil Infrastructure Engineering*; Springer: Berlin/Heidelberg, Germany, 2016; Chapter 9.
5. Ayan, A.; Senturk, A.E. Exploring of Biomass Energy Specific to Turkey and on a Global Scale. *Int. J. Renew. Energy Res.* **2023**, *13*, 1456–1472. [CrossRef]
6. Smart Güneş Enerjisi Teknolojileri Araştırma Geliştirme Üretim Sanayi ve Ticaret Anonim Şirketi. Faaliyet Raporu 2023. Available online: https://www.smartsolar.com.tr/ (accessed on 30 May 2024).
7. IEA. *World Energy Outlook 2023*; International Energy Agency: Paris, France, 2023; Available online: https://www.iea.org/reports/world-energy-outlook-2023 (accessed on 30 May 2024).
8. IEA; IRENA; UN. *Climate Change High-Level Champions. Breakthrough Agenda Report 2023: Accelerating Sector Transitions Through Stronger International Collaboration*; International Energy Agency: Paris, France, 2023; Available online: https://www.iea.org/reports/breakthrough-agenda-report-2023 (accessed on 30 May 2024).
9. Fathy, A.M.; Abdelhady, M.I.; Juma, F. The Architectural Tools in Reducing Energy Consumption of Residential Buildings in Hot Countries. *Int. J. Appl. Eng. Res.* **2020**, *15*, 135–143.
10. Turhan, C.; Ghazi, S. Energy Consumption and Thermal Comfort Investigation and Retrofitting Strategies for an Educational Building: Case Study in a Temperate Climate Zone. *J. Build. Des. Environ.* **2023**, *2*, 16869. [CrossRef]
11. Duzgun, B.; Aydinalp Koksal, M.; Bayindir, R. Assessing Drivers of Residential Energy Consumption in Turkey: 2000–2018. *Int. J. Appl. Eng. Res.* **2022**, *17*, 135–143. [CrossRef]
12. Bilgili, M.; Şahin, B.; Kahraman, A. Wind energy potential in Antakya and İskenderun regions, Turkey. *Renew. Energy* **2004**, *29*, 1733–1745. [CrossRef]
13. Saygin, D.; Hoffman, M.; Godron, P. How Turkey Can Ensure a Successful Energy Transition. Center for American Progress. July 2018. Available online: www.americanprogress.org (accessed on 20 April 2024).
14. Acar, A.; Güllü, A.B.; Aksoy, H.; Çalışkan, R.Y.; Serhadlıoğlu, S.; Taranto, Y. *Türkiye Enerji Dönüşümü Görünümü 2023*; SHURA Enerji Dönüşümü Merkezi, Sabancı Üniversitesi: Istanbul, Turkey, 2024; ISBN 978-625-6956-40-7. Available online: https://www.shura.org.tr (accessed on 10 May 2024).

15. International Energy Agency (IEA). *Energy Policy Review Turkey 2021*; IEA: Paris, France, 2021; Available online: www.iea.org/reports/energy-policy-review-turkey-2021 (accessed on 20 April 2024).
16. Salhein, K.; Kobus, C.J.; Zhody, M. Forecasting Installation Capacity for the Top 10 Countries Utilizing Geothermal Energy by 2030. *Thermo* **2022**, *2*, 334–351. [CrossRef]
17. PwC Türkiye. *Dünyada ve Türkiye'de Güneş Enerjisi Sektörü*; PwC: Mart, TX, USA, 2024; Available online: http://www.pwc.com.tr/ (accessed on 30 May 2024).
18. IRENA. *World Energy Transitions Outlook 2023: 1.5 °C Pathway*; International Renewable Energy Agency: Abu Dhabi, United Arab Emirates, 2023; ISBN 978-92-9260-527-8. Available online: https://www.irena.org/publications (accessed on 30 May 2024).
19. Varolgüneş, F.K. Post-disaster permanent housing: The case of the 2003 Bingöl earthquake in Turkey. *Disaster Prev. Manag. Int. J.* **2021**, *30*, 175–189. [CrossRef]
20. Yön, B. Identification of failure mechanisms in existing unreinforced masonry buildings in rural areas after 4 April 2019 earthquake in Turkey. *J. Build. Eng.* **2021**, *43*, 102586. [CrossRef]
21. Ozmen, H.B. A view on how to mitigate earthquake damages in Turkey from a civil engineering perspective. *Res. Eng. Struct. Mater.* **2021**, *7*, 1–11. [CrossRef]
22. Işık, E.; Büyüksaraç, A.; Ekinci, Y.L.; Aydın, M.C.; Harirchian, E. The Effect of Site-Specific Design Spectrum on Earthquake-Building Parameters: A Case Study from the Marmara Region (NW Turkey). *Appl. Sci.* **2020**, *10*, 7247. [CrossRef]
23. Aman, D.D.; Aytac, G. Multi-criteria decision making for city-scale infrastructure of post-earthquake assembly areas: Case study of Istanbul. *Int. J. Disaster Risk Reduct.* **2022**, *67*, 102668. [CrossRef]
24. Atmaca, B.; Demir, S.; Günaydın, M.; Altunışık, A.C.; Hüsem, M.; Ateş, Ş.; Adanur, S.; Angın, Z. Lessons learned from the past earthquakes on building performance in Turkey. *J. Struct. Eng. Appl. Mech.* **2020**, *3*, 61–84. [CrossRef]
25. Ozturk, M.; Arslan, M.H.; Dogan, G.; Ecemis, A.S.; Arslan, H.D. School buildings performance in 7.7 Mw and 7.6 Mw catastrophic earthquakes in southeast of Turkey. *J. Build. Eng.* **2023**, *79*, 107810. [CrossRef]
26. Ozturk, M.; Arslan, M.H.; Korkmaz, H.H. Effect on RC buildings of 6 February 2023 Turkey earthquake doublets and new doctrines for seismic design. *Eng. Fail. Anal.* **2023**, *153*, 107521. [CrossRef]
27. Tao, W.; Jie, C.; Yujiang, Z.; Xiaoqing, W.; Xuchuan, L.; Xiaoting, W.; Qingxue, S. Preliminary investigation of building damage in Hatay under February 6, 2023 Turkey earthquakes. *Earthq. Eng. Eng. Vib.* **2023**, *22*, 1010. [CrossRef]
28. Alrwashdeh, S.S. Investigation of the energy output from PV panels based on using different orientation systems in Amman-Jordan. *Case Stud. Therm. Eng.* **2021**, *28*, 101580. [CrossRef]
29. Burg, B.R.; Ruch, P.; Paredes, S.; Michel, B. Effects of radiative forcing of building integrated photovoltaic systems in different urban climates. *Sol. Energy* **2017**, *147*, 399–405. [CrossRef]
30. Biyik, E.; Araz, M.; Hepbasli, A.; Shahrestani, M.; Yao, R.; Shao, L.; Essah, E.; Oliveira, A.C.; Del Caño, T.; Rico, E.; et al. A key review of building integrated photovoltaic (BIPV) systems. *Eng. Sci. Technol. Int. J.* **2017**, *20*, 833–858. [CrossRef]
31. Maghrabie, H.M.; Elsaid, K.; Sayed, E.T.; Abdelkareem, M.A.; Wilberforce, T.; Olabi, A.G. Building-integrated photovoltaic/thermal (BIPVT) systems: Applications and challenges. *Sustain. Energy Technol. Assess.* **2021**, *45*, 101151. [CrossRef]
32. Topal, A.; Özoğlu, B.; Ekşioğlu, D. The evaluation of factors in utilizing the potential of solar energy: The case of Turkey. *Environ. Res. Technol.* **2021**, *4*, 266–276. [CrossRef]
33. Çeçen, M.; Yavuz, C.; Aksoy Tırmıkçı, C.; Sarıkaya, S.; Yanıkoğlu, E. Analysis and evaluation of distributed photovoltaic generation in electrical energy production and related regulations of Turkey. *Clean Technol. Environ. Policy* **2022**, *24*, 1321–1336. [CrossRef] [PubMed]
34. Hajizadeh, S.; Seyis, S. Retrofit strategies for a nearly-zero energy residential building: A case study in Antalya, Türkiye. In Proceedings of the 3rd International Civil Engineering and Architecture Congress (ICEARC'23), Antalya, Türkiye, 12–14 October 2023; pp. 1–12. [CrossRef]
35. Adan, H.K.; Filik, Ü.B. Performance Investigation of On-Grid Solar Photovoltaic System in Eskişehir/Turkey. *DEÜ FMD* **2021**, *23*, 557–566. [CrossRef]
36. Turhan, C.; Saleh, Y.A.S. A Case Study for Small-Scale Vertical Wind Turbine Integrated Building Energy Saving Potential. *J. Build. Des. Environ.* **2024**, *3*, 28115. [CrossRef]
37. Kottek, M.; Grieser, J.; Beck, C.; Rudolf, B.; Rubel, F. World Map of the Köppen-Geiger Climate Classification Updated. *Meteorol. Z.* **2006**, *15*, 259–263. [CrossRef] [PubMed]
38. Zengin, G.; Koç, A.; Artaş, S.B.; Köse, Ö.; Koç, Y.; Yağlı, H. Comparative Analyses of the Solar Energy Potentials of Gaziantep, Konya and Hatay: A Case Study for 1 MW of Photovoltaic System. *Int. J. Energy Eng. Sci.* **2024**, *9*, 1–11.
39. Global Wind Atlas. Available online: https://globalwindatlas.info/ar (accessed on 13 April 2024).
40. Türk Standardları Enstitüsü. *TS 825: Thermal Insulation Requirements for Buildings*; Türk Standardları Enstitüsü: Ankara, Turkey, 2008; Available online: https://intweb.tse.org.tr (accessed on 2 May 2024).
41. DesignBuilder Software Ltd. DesignBuilder, v.6.1.0.006. Available online: http://www.designbuilder.co.uk/ (accessed on 8 May 2024).
42. SolidWorks. 2018. Available online: https://www.solidworks.com/ (accessed on 10 May 2024).
43. ANSYS, Inc. ANSYS Fluent. 2020. Available online: https://www.ansys.com/ (accessed on 10 May 2024).

44. Eltayesh, A.; Castellani, F.; Natili, F.; Burlando, M.; Khedr, A. Aerodynamic upgrades of a Darrieus vertical axis small wind turbine. *Energy Sustain. Dev.* **2023**, *73*, 126–143. [CrossRef]
45. Zidane, I.F.; Ali, H.M.; Swadener, G.; Eldrainy, Y.A.; Shehata, A.I. Effect of Upstream Deflector Utilization on H-Darrieus Wind Turbine Performance: An Optimization Study. *Alex. Eng. J.* **2023**, *63*, 175–189. [CrossRef]

Disclaimer/Publisher's Note: The statements, opinions and data contained in all publications are solely those of the individual author(s) and contributor(s) and not of MDPI and/or the editor(s). MDPI and/or the editor(s) disclaim responsibility for any injury to people or property resulting from any ideas, methods, instructions or products referred to in the content.